Available online at www.sciencedirect.com
SCIENCE DIRECT®
Catalysis Today 97 (2004) 233–240
CATALYSIS TODAY
www.elsevier.com/locate/cattod

# Synthesis, characterization and catalytic properties of benzyl sulphonic acid functionalized Zr-TMS catalysts

Surendran Parambadath, M. Chidambaram, A.P. Singh*

*Catalysis Division, National Chemical Laboratory, Pune 411008, India*

Available online 11 September 2004

**Abstract**

Mesoporous zirconium hydroxide, Zr-TMS (zirconium hydroxide with mesostructured framework; TMS, transition metal oxide mesoporous molecular sieves) catalyst has been prepared through the sol–gel method and functionalized with benzyl sulphonic acid (BSA) using post-synthesis route without destroying the mesoporous structure. The benzyl group anchored Zr-TMS (B-Zr-TMS/≡Zr–O–$CH_2$–Φ) was achieved by etherification reaction of Zr-TMS with benzyl alcohol at 80 °C using cyclohexane as solvent. Further, B-Zr-TMS was subjected to sulphonation reaction with chlorosulphonic acid ($ClSO_3H$) at 70 °C using chloroform as solvent to yield BSA-Zr-TMS (≡Zr–O–$CH_2$–Φ–$SO_3H$). Maximum sulphonic acid (–$SO_3H$) loading was optimized with respect to time of functionalization and concentration of $ClSO_3H$. Functionalization was carried out by loading the maximum amount of benzyl group over Zr-TMS and varying the concentration of –$SO_3H$. The synthesized materials have been characterized by powder XRD, FT-IR, elemental analysis, $N_2$ adsorption–desorption and TPD of ammonia. The catalytic activity of the synthesized catalyst has been performed in liquid phase benzoylation of diphenyl ether to 4-phenoxybenzophenone (4-PBP) using benzoyl chloride as benzoylating agent at 160 °C under atmospheric pressure. The same reaction was carried out by sulphated zirconia ($SO_4^{2-}/ZrO_2$) and found very poor activity.


*Keywords:* B-Zr-TMS; BSA-Zr-TMS; Benzyl sulphonic acid; Functionalization; Benzoylation of diphenyl ether

## 1. Introduction

The Mobil researchers opened a new area in the synthesis of mesoporous materials through the discovery of M41S family of silicate mesoporous molecular sieves, particularly, MCM-41 by liquid-crystal templating mechanism [1]. Because of thermal stability, high surface area (around 1000 $m^2/g$) and narrow pore-size distribution, these materials have invited a great deal of attention for the synthesis of wide range of bulky organic molecules. However, the MCM-41 type materials showed weak acid sites [2]. The synthesis of transition metal oxide based mesoporous materials such as titania, niobia, tantala, zirconia, alumina, manganese oxide, ceria, hafnia and chromia were attempted [3]. Among these materials, zirconia and alumina, only maintain the mesoporous structure upon the removal of template from the material by calcination or solvent extraction methods. Further, among the mesoporous materials, zirconia is of particular interest due to the high thermal stability and ease of synthesis [4,5]. Because of the various oxidation states of zirconia, in addition to the high surface area, moderate acidity and the attractive porous nature have advantages over aluminosilicate materials for use in electromagnetics, photoelectronics and as a good support in catalysis [6]. The bifunctional nature of mesoporous zirconia has an unusual interest in the field of acidic catalysis. However, many attempts have been made to increase the acidity of these materials by using dopants or functional groups. Doping phosphates [7] or sulfates [8] result not only in an increase in the acidity but also a relative increase in thermal stability. These attempts result the preparation of mesoporous sulfated zirconia having partially tetragonal wall structure and narrow distribution of pore sizes by controlled hydrolysis of zirconium propoxide [9]. Moreover, the addition of the sulfate ion stabilizes the mesoporous morphology and delays crystallization. MCM-41 analogous materials have been synthesized together with zirconium

* Corresponding author. Tel.: +91 20 25893761; fax: +91 20 25893761.
*E-mail address:* apsingh@cata.ncl.res.in (A.P. Singh).

0920-5861/$ – see front matter © 2004 Elsevier B.V. All rights reserved.
doi:10.1016/j.cattod.2004.07.007

oxide-sulfate and zirconium oxo phosphate [10] and a special post-synthetic treatment has been developed in the later case. In recent years, sulphonic acid functionalized mesoporous materials have been used in a variety of reactions such as condensation [11], esterifications [12–16] and acylation [17] reactions. Sulphonic acid functionalized MCM-41 [16], SBA-2 [14] and SBA-15 [15,18] were prepared through a thiol oxidation route. As a result, one-pot sol–gel route has been employed to achieve high levels of (3-mercaptopropyl)trimethoxysilane (3-MPTS) incorporation into mesoporous silica with >90% efficiency and characterized by XPS and Raman spectroscopy [11]. Among the functionalized MCM-41 type materials, phenyl sulphonic acid functionalized MCM-41 exhibits better performance than the alkyl sulphonic acid functionalized MCM-41 in the esterification reactions. Using both catalysts, the esterification of glycerol with lauric acid and oleic acid were studied by Mohino et al. [12,16]. Sohn et al. [19] reported a modified silica catalyst with derivatives of benzene-sulfonate groups and studied the catalytic activity in dehydration reactions. In order to establish novel environmentally benign materials, trifluoromethanesulphonic acid functionalized mesoporous zirconia was synthesized in our laboratory using a post-synthetic method and the activity of the functionalized materials was tested in the benzoylation of biphenyl to 4-phenylbenzophenone and acetalization of ethylacetoacetate to fructone [17].

In the present work, we investigated the functionalization of benzyl group loaded mesoporous zirconium hydroxide with various amounts of chlorosulphonic acid without damaging the mesostructure of Zr-TMS. The functionalized materials were characterized by various physico-chemical techniques. The performance of the catalysts was tested in the benzoylation of diphenyl ether and the results were compared with the $SO_4^{2-}/ZrO_2$.

## 2. Experimental

### 2.1. Catalyst preparation

#### 2.1.1. Synthesis of Zr-TMS

The Zr-TMS was synthesized by adopting the following molar composition, $0.1Zr(OC_4H_9)_4$:1.4BuOH:0.025CTMABr:0.03TMAOH:4 $H_2O$:0.05Acac:0.5EtOH.

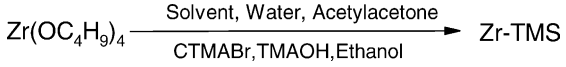


Scheme 1.

Mesoporous zirconium hydroxide (Zr-TMS) was synthesized by sol–gel route [9] using zirconium butoxide (80 wt.% solution in 1-butanol, Aldrich, USA) as the zirconia source and *N*-cetyl-*N*,*N*,*N*-trimethyl ammonium bromide (CTMABr, S.d.fine-Chem. Ltd., India) as surfactant at a pH of 11.5, which was maintained by tetramethyl ammonium hydroxide (TMAOH 25 wt.% aq. solution, S.d.fine-Chem. Ltd.) solution. Acetylacetone (Acac) and ethanol controlled the rate of hydrolysis of zirconium butoxide in water. In a mixture of water (4 mol) and TMAOH (0.03 mol), CTMABr (0.025 mol) was dissolved and stirred for 1 h. Then, a mixture of zirconium butoxide (0.1 mol), acetylacetone (0.05 mol) and ethanol (0.5 mol) were added to the template solution slowly and allowed to stir for 3 h. Further, the mixture was refluxed under stirring for 48 at 90 °C. The resulting solid was filtered, washed with acetone and dried for 10 h at 100 °C (Scheme 1).

#### 2.1.2. Surfactant removal

The solvent extraction method was employed to remove the template from the pores of the mesostructure without destroying the structure of the molecular sieves using ethanol and HCl mixture. The efficiency of the process was confirmed by elemental analysis and powder X-ray diffraction studies. One gram as-synthesized Zr-TMS was taken and refluxed with a mixture of 100 g of distilled ethanol and 1 g of conc. HCl (36 wt.%) for 6, 8 and 10 h at 80 °C. Fresh samples were used for each extraction. The extracted samples were washed several times with pure distilled ethanol and acetone. The resulting solid was dried at 100 °C for 10 h.

#### 2.1.3. Synthesis of functionalized mesoporous BSA-Zr-TMS

In the first step, the functionalization of benzyl alcohol (0.1 mol, Merck) over Zr-TMS (10 g) was carried out by etherification reaction using cyclohexane (0.35 mol, Thomas Baker, India) as solvent at 80 °C for 10 h (Scheme 2). The sample was filtered and washed with cyclohexane, benzene and finally with acetone and dried for 6 h at 50 °C. To protect the unloaded hydroxyl groups, after modification

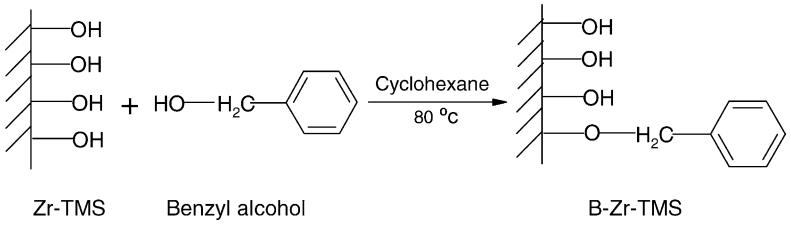


Scheme 2. Etherification.

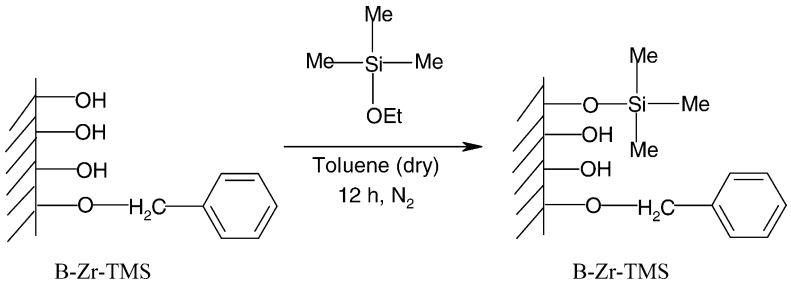


B-Zr-TMS B-Zr-TMS

Scheme 3. Silylation.

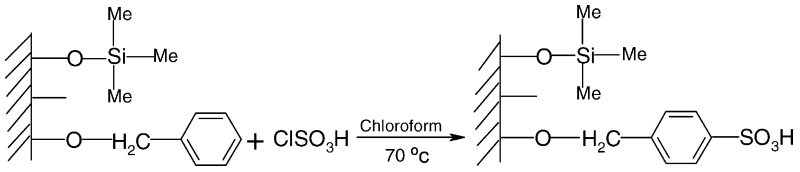


B-Zr-TMS BSA-Zr-TMS

Scheme 4. Sulphonation.

with benzyl alcohol, desired amount of B-Zr-TMS was degassed at 80 °C for 2 h and dry toluene was added. Then, an excess of ethoxytrimethyl-silane was added and the suspension was refluxed at 70 °C under nitrogen atmosphere for 12 h (Scheme 3). The solid was filtered and soxhlet extraction was done with dichloromethane for 12 h and dried at 50 °C for 5 h. Further, sulphonation of the resulting material, B-Zr-TMS was done with the appropriate amount of chlorosulphonic acid (Spectrochem, India) using chloroform (0.12 mol, Merck India) as solvent at 70 °C for 3 h (Scheme 4). The chlorosulphonic acid was added slowly sulphonation by a syringe to the mixture of B-Zr-TMS and chloroform. Thus the material obtained was washed with chloroform and soxhlet extraction was done with a mixture of 1:1 diethyl ether and dichloromethane and dried at 50 °C for 6 h. Benzyl alcohol and sulphonic acid functionalized B-Zr-TMS are designated as, B-Zr-TMS and BSA-Zr-TMS, respectively.

$SO_4^{2-}/ZrO_2$ was obtained from MEL Chemicals, Manchester, UK and activated at 500 °C for 10 h under static air prior to reaction.

### 2.2. Catalyst characterization

In order to identify the structure and phase purity, powder X-ray diffraction analysis was done on a Rigaku D-max III VC; X-ray diffractometer with Ni filtered Cu Kα radiation having curved graphite crystal monochromator and NaI scintillation counter. Porosity and surface area measurements were performed following $N_2$ adsorption on a Quantachrome NOVA 2000 instrument with high vacuum. The BET method was used for the calculation of surface area. For this particular measurement, the samples were activated at 150 °C for 3 h under vacuum and then the adsorption–desorption was conducted by passing nitrogen onto the sample, which was kept under liquid nitrogen. The elemental analyses were done with an EA1108 CHN/S elemental analyzer (Carlo Erba Instrument) for establishing the presence and exact fraction of elements in the synthesized materials. A Shimadzu FT-IR 8201 PC was used to probe the functionalized groups in the material using diffuse reflectance spectroscopy. TPD of ammonia was used to find out the number and nature of the acidic sites present in the catalyst [17].

### 2.3. Catalytic reaction experiments

Benzoylation of diphenyl ether (DPE) with benzoyl chloride (BC) has been used to study the catalytic performance of the catalysts in a batch reactor using nitrobenzene (NB) as solvent at 160 °C (Scheme 5). 1:1 molar ratio (0.01 mol each) of diphenyl ether (S.d.fine-Chem. Ltd.) and benzoyl chloride (S.d.fine-Chem. Ltd.) were taken along with nitrobenzene (S.d.fine-Chem. Ltd.) in a 50 ml two-necked round bottom flask attached to a condenser and a septum. A required amount of activated catalyst (0.5 g) was added to the reaction mixture. An oil bath is used to maintain the reaction temperature at 160 °C. The reaction mixture was withdrawn by syringe at various

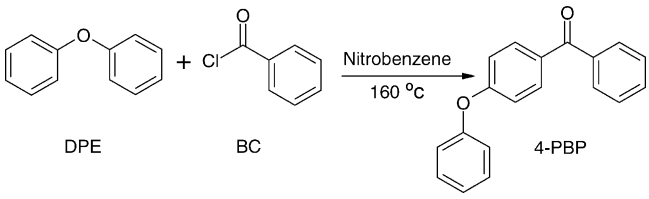


DPE BC 4-PBP

Scheme 5. Benzoylation of DPE.

time of intervals and analyzed by a gas chromatograph (HP 6890) equipped with a flame ionization detector (FID) and a capillary column (HP, 5 μm thick cross-linked methyl silicone gum, 0.2 mm × 50 m). The product was identified by injecting authentic samples in gas-chromatograph and by GC–MS (Shimadzu 2000 A) analysis. The geometry optimization of diphenyl ether has been done by performing a restricted Hartree–Fock (RHF) calculation using a STO-3G basis set. The calculations are done in Gamess US ab initio quantum chemistry package.

## 3. Results and discussion

### 3.1. Catalyst characterization

#### 3.1.1. Powder X-ray diffraction study

*3.1.1.1. Optimization of template extraction.* Fig. 1 shows the powder XRD pattern of as-synthesized Zr-TMS, and different time of extraction (such as 6, 8 and 10 h) to remove the template from the synthesized Zr-TMS for establishing the time of extraction without destroying the mesoporous structure. All spectra show a sharp peak at low $2\theta$ (2°–4°) range, which is characteristic of ordered porous structure of Zr-TMS, and two broad peaks at 30° (broad) and 50° (small), which are attributed to the amorphous nature of $Zr(OH)_4$ [20]. Further, when it is calcined above 500 °C it may give sharp and intense peaks characteristic of tetragonal, monoclinic and cubic phases of $ZrO_2$, which are not shown here. The intensity of mesophase decreases with the increase in time of extraction. The decrease in intensity of Zr-TMS with the increase in time of extraction is attributed to the partial structure damage of Zr-TMS. The surface areas of these samples, 6, 8 and 10 h (Fig. 1) were found to be 341, 370 and 364 $m^2/g$, respectively. The surface area measurement revealed that after 6 h of extraction, the sample was partially extracted. Though the 8 and 10 h samples did not show much difference in surface area but the XRD intensity of 10 h sample decreased (Fig. 1) indicating that there is a structure damage to some extent and hence it is clear that 8 h extraction is the optimum time for removal of template from the synthesized material.

*3.1.1.2. Influence of time of $ClSO_3H$ functionalization.* The influence of time of chlorosulphonic acid functionalization on the mesoporous nature of BSA-Zr-TMS catalyst is shown in Fig. 2 (B-Zr-TMS, 1, 2, 3, 3.5, 4 and 4.5 h). Ten wt.% chlorosulphonic acid was used over B-Zr-TMS to optimize the time without the structure collapse. The intensity of the mesophase in all the samples at low $2\theta$ range (characteristic for mesoporous material) decreases with the increase in functionalization time, which showed that there was slow decay of mesoporous nature. Further, XRD pattern shows that after 3 h of reflux time extra peaks were noticed, which may be the prominent phases of zirconia, such as tetragonal, monoclinic and cubic. The

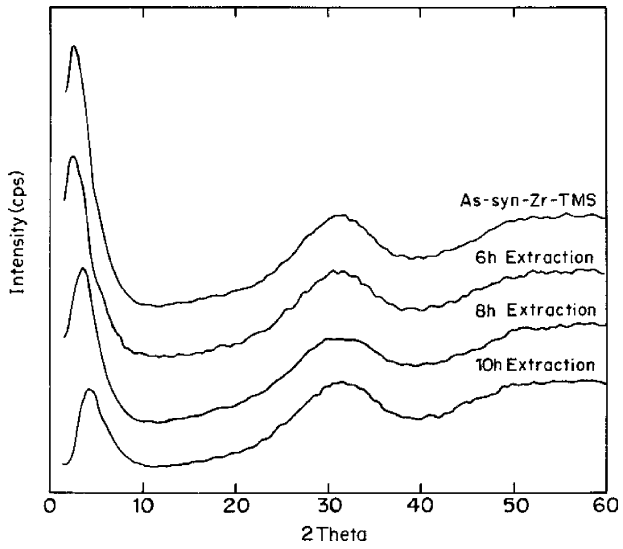


Fig. 1. Powder XRD pattern of Zr-TMS with respect to template extraction time As-syn Zr-TMS, 6, 8 and 10 h.

intensity of these peaks increased with the increase in reflux time (Fig. 2, 4 and 4.5 h), which revealed that there was fast crystallization and consequently severe structure damage of the material. The surface area of B-Zr-TMS, 1, 2, 3, 3.5, 4 and 4.5 h samples were found to be 308, 287, 229, 215, 201, 181 and 172 $m^2/g$, respectively. The decrease in surface area may be attributed to the loading of $–SO_3H$ group over B-Zr-TMS and a decrease in mesophase of B-Zr-TMS may be due to the formation of HCl as by product during functionalization, which destroys the mesoporous structure to some extent. It is clear from these data that time of functionalization cannot be extended beyond 3 h at our experimental condition to get optimum concentration of sulphonic acid over B-Zr-TMS.

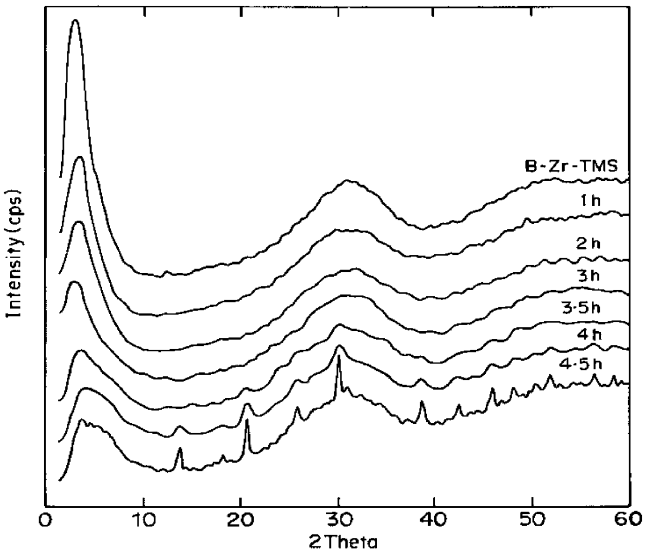


Fig. 2. Powder XRD pattern of standardization of $ClSO_3H$ functionalization over B-Zr-TMS with respect to time.

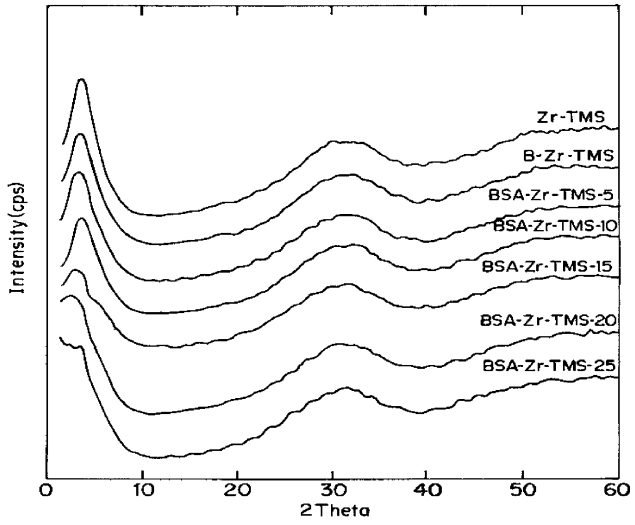


Fig. 3. Powder XRD pattern of Zr-TMS, B-Zr-TMS and different loadings of sulphonic acid over B-Zr-TMS catalyst.

*3.1.1.3. Influence of concentration of sulphonic acid.* Fig. 3 illustrates Zr-TMS, B-Zr-TMS and the influence of $ClSO_3H$ concentration over B-Zr-TMS (BSA-Zr-TMS-5, -10, -15, -20 and -25). The functionalization of B-Zr-TMS by $ClSO_3H$ was done by varying the concentration of $ClSO_3H$ and keeping the functionalization time at 3 h. Various loading of sulphonic acid over B-Zr-TMS such as 5, 10, 15, 20 and 25 wt.% (input) was done and found to be 4.7, 9.1, 10.3, 11.6 and 12 wt.% (output) of $SO_3H$ over B-Zr-TMS, respectively (see Table 1, elemental analysis). The crystallinity of the sulphonic acid containing B-Zr-TMS materials decreased as the chlorosulphonic acid loading increased. Moreover, once the concentration of chlorosulphonic acid was increased >15 wt.% (see Fig. 3) the mesophase started to vanish and it was observed that at higher loading (25 wt.%, BSA-Zr-TMS-25) the structure was completely destroyed. The surface areas of Zr-TMS, B-Zr-TMS, BSA-Zr-TMS-5, BSA-Zr-TMS-10, BSA-Zr-TMS-15, BSA-Zr-TMS-20 and BSA-Zr-TMS-25 were found to be 370, 308, 229, 198, 179, 158 and 98 $m^2/g$, respectively (Table 1). A decrease in surface area of BSA-Zr-TMS may be attributed to the sulphonic acid loading and due to the formation of HCl as by product during functionalization. The above results demonstrate that the B-Zr-TMS can accommodate a maximum of 9.1 wt.% of sulphonic acid at our experimental condition without destroying the mesostructure.

*3.1.2. Nitrogen adsorption–desorption study*

Incorporation or anchoring of any medium (acid or base) or metal in the framework positions and/or into the walls of the supporting medium leads to a progressive decrease in surface area [21]. The BET surface area of the Zr-TMS, B-Zr-TMS, BSA-Zr-TMS and $SO_4^{2-}/ZrO_2$ are given in Table 1. The surface area for the Zr-TMS was 370 $m^2/g$, which is comparable to that measured previously for a Zr-TMS synthesized using a surfactant with $C_{16}$ carbon chain [22]. The surface area gradually decreased with increasing sulphonic acid loading.

Fig. 4 A, B and C show the nitrogen adsorption–desorption isotherm of Zr-TMS, B-Zr-TMS and BSA-Zr-TMS-10 (10 represents the input concentration of sulphonic acid over B-Zr-TMS), respectively. All the three isotherms are of type IV characteristic of mesoporous materials. Position of inflection of BSA-Zr-TMS-10 shows that there is structure damage in the materials. However, pore size

Table 1
Physico-chemical properties of synthesized catalysts

| Catalyst | Elemental analysis (output)[a] (wt.%) | | Loading of sulphonic acid (wt.%) | | BET surface area ($m^2/g$)[b] | $NH_3$ desorbed (mmol/g) | | | | $NH_3$ chemi-sorbed at 30 °C (mmol/g)[c] |
|---|---|---|---|---|---|---|---|---|---|---|
| | C | S | Input | Output | | 30–70 °C | 70–110 °C | 110–150 °C | 150–200 °C | |
| Zr-TMS[d] | – | – | – | – | 370 | 0.06 | 0.15 | 0.19 | 0.10 | 0.50 |
| B-Zr-TMS[e] | – | – | – | – | 308 | – | – | – | – | – |
| BSA-Zr-TMS-5[f] | 2.9 | 2.0 | 5 | 4.7 | 229 | 0.11 | 0.26 | 0.31 | 0.04 | 0.72 |
| BSA-Zr-TMS-10[g] | 1.6 | 2.5 | 10 | 9.1 | 198 | 0.23 | 0.38 | 0.41 | 0.17 | 1.19 |
| BSA-Zr-TMS-15 | 1.1 | 2.8 | 15 | 10.3 | 179 | 0.22 | 0.39 | 0.43 | 0.18 | 1.22 |
| BSA-Zr-TMS-20 | 0.9 | 3.2 | 20 | 11.6 | 158 | 0.25 | 0.40 | 0.46 | 0.20 | 1.31 |
| BSA-Zr-TMS-25 | 0.7 | 3.3 | 25 | 12.0 | 98 | 0.25 | 0.41 | 0.48 | 0.20 | 1.34 |
| $SO_4^{2-}/ZrO_2$[h] | – | 2.6 | 10 | 7.9 | 101 | – | – | – | – | 1.45[i] |

[a] Measured by EA 1108 CHN/S elemental analyzer to measure the acid loading.
[b] Measured by $N_2$ adsorption–desorption at −196 °C.
[c] Total acid sites determined in the solid catalyst by $NH_3$ adsorption–desorption from 30 to 200 °C.
[d] Total pore volume is 0.31 $cm^3/g$, average pore diameter is 30.9 Å for Zr-TMS.
[e] Total pore volume is 0.28 $cm^3/g$, average pore diameter is 26.4 Å for B-Zr-TMS.
[f] Numbers denote wt.% (input) of sulphonic acid loading over B-Zr-TMS.
[g] Total pore volume is 0.18 $cm^3/g$, average pore diameter is 18.2 Å for BSA-Zr-TMS-10.
[h] Total pore volume is 0.09 $cm^3/g$, average pore diameter is 9 Å for $SO_4^{2-}/ZrO_2$.
[i] Ammonia desorbed from 30 to 500 °C in six steps.

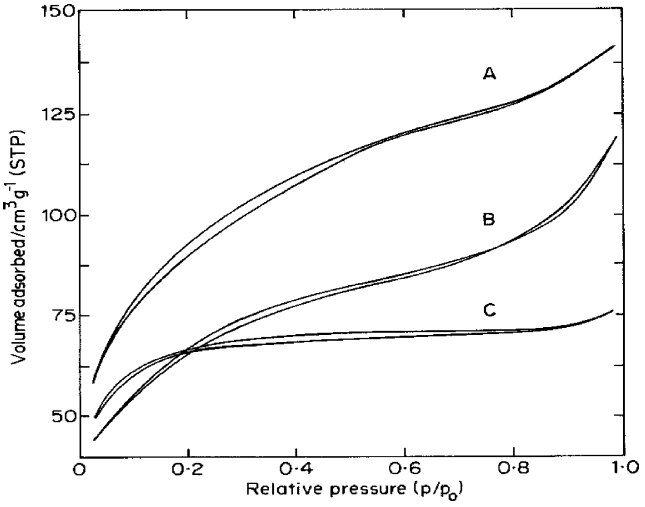


Fig. 4. $N_2$ adsorption–desorption isotherms of: (A) Zr-TMS, (B) B-Zr-TMS and (C) BSA-Zr-TMS-10.

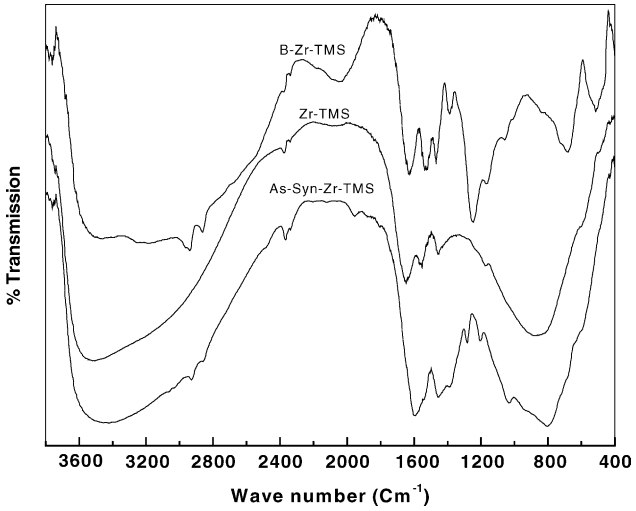


Fig. 6. FT-IR spectra of As-syn-Zr-TMS, Zr-TMS and B-Zr-TMS.

distribution analysis indicates that mesoporosity was not lost.

Fig. 5 A, B and C show the BJH pore size distribution curves of Zr-TMS, B-Zr-TMS and BSA-Zr-TMS-10. The surface area, total pore volume and average pore diameter of the Zr-TMS, B-Zr-TMS and BSA-Zr-TMS-10 were found to be 370 $m^2$/g, 0.31 $cm^3$/g, 30.9 Å; 308 $cm^2$/g, 0.28 $cm^3$/g, 26.4 Å and 198 $m^2$/g, 0.18 $cm^3$/g, 18.2 Å, respectively (Table 1). These results demonstrate that the surface area, pore volume and pore diameter of the functionalized materials decrease [21,22] due to the anchoring of benzyl group over Zr-TMS and further functionalization of B-Zr-TMS with $ClSO_3H$. The surface area, pore volume and average pore diameter of $SO_4^{2-}/ZrO_2$ are found to be 101 $m^2$/g, 0.09 $cm^3$/g and 9 Å (Table 1), respectively, which shows that this material is not suitable for this particular reaction (benzoylation of diphenyl ether) because of the bulky nature of the product (4-PBP).

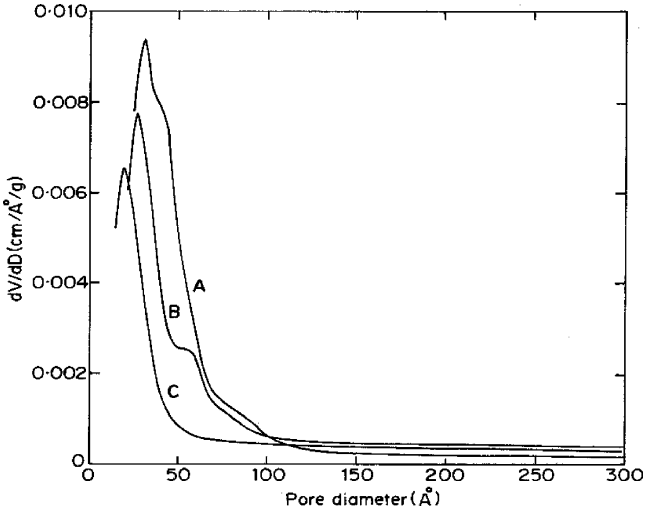


Fig. 5. BJH pore size distributions of: (A) Zr-TMS, (B) B-Zr-TMS and (C) BSA-Zr-TMS-10.

*3.1.3. FT-IR study*

The infrared spectra of as-synthesized-Zr-TMS, Zr-TMS and B-Zr-TMS are shown in Fig. 6. In all the spectra, a weak unresolved band between 900 and 750 $cm^{-1}$ is attributed to Zr–O stretching vibrations [17]. A broad band between 3400 and 3650 $cm^{-1}$ corresponds to the O–H stretching vibration in $Zr(OH)_4$ and a sharp band between 1650 and 1600 $cm^{-1}$ is due to the bending vibrations of surface O–H groups and water molecules occluded in the pores [23].

In addition to the above bands, the as-synthesized Zr-TMS shows the additional weak bands at around 3200–2800 and 1500–1300 $cm^{-1}$ which are due to the C–H stretching and bending vibrations [24] of methylene group of template material. These bands are absent in the template extracted Zr-TMS, which shows that the template removal by ethanol and HCl mixture is complete and successful. After loading of benzyl alcohol over Zr-TMS (B-Zr-TMS or ≡Zr–O–$CH_2$–Φ), the weak bands at around 3200–2800 $cm^{-1}$ and 1500–1300 $cm^{-1}$ are due to the C–H stretching and bending vibrations [24] of methylene group as discussed earlier and a medium band at 1423 $cm^{-1}$ indicates the C=C stretching [24] in-plane vibration of benzene framework. A band at 707$cm^{-1}$ represents the C–H bending vibration of methylene group of benzene [24]. A small and weak band at around 1000–1200 $cm^{-1}$ is the characteristic band of C–O group in the catalyst.

The FT-IR spectra of two loadings (5 and 10 wt.% $ClSO_3H$) of sulphonic acid functionalized B-Zr-TMS (BSA-Zr-TMS-5 and BSA-Zr-TMS-10) are shown in Fig. 7. A small and intense band at 1298 $cm^{-1}$ and the medium band at 1185 $cm^{-1}$, are due to S=O stretching mode of incorporated sulphonic acid [17]. The C=S link also gives a medium band between 600 and 700 $cm^{-1}$ and the intensity is increased with the increase in acid loading.

Further, it is noticed that the intensity of the stretching and bending modes of –C–H group remained unchanged in B-Zr-TMS, BSA-Zr-TMS-5 and BSA-Zr-TMS-10 with the

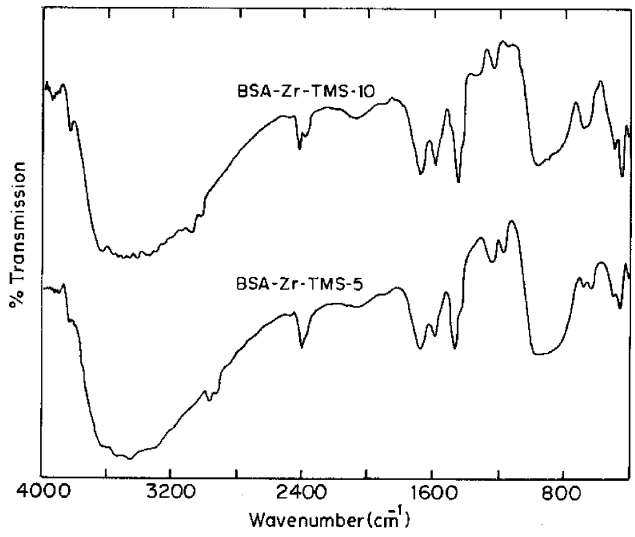


Fig. 7. FT-IR spectra of BSA-Zr-TMS-5 and BSA-Zr-TMS-10.

increase in sulphonic acid loading, which shows that the attachment of $-SO_3H$ is on the benzene ring. These observations confirm the successful anchoring of benzyl group over Zr-TMS to B-Zr-TMS and its functionalization with $ClSO_3H$ to BSA-Zr-TMS.

### 3.1.4. Ammonia adsorption–desorption study

Temperature programmed desorption (TPD) of ammonia was performed for measuring the total acidity (acid sites) of the synthesized materials ([17] and references therein). The results of the stepwise desorption of ammonia of Zr-TMS, BSA-Zr-TMS and $SO_4^{2-}/ZrO_2$ are presented in Table 1. The values of acidity for Zr-TMS and functionalized Zr-TMS were obtained by desorbing ammonia in four stages from 30 to 200 °C (between 30 and 70 °C, 70 and 110 °C, 110 and 150 °C, and 150 and 200 °C). Since the functionalized material is covalently bonded to the solid support, it could not be treated above 200 °C, which is evidenced by thermal analysis (not shown here). Above this temperature, benzyl sulphonic acid is lost from the solid support. Whereas, the adsorbed ammonia from $SO_4^{2-}/ZrO_2$ was desorbed in six stages between 30 and 500 °C.

The results reveal that the total acidity and the acid site distribution are dependent on the type of catalyst and are strongly influenced by the amount of sulphonic acid loading over B-Zr-TMS. The total acidity of Zr-TMS, BSA-Zr-TMS-5, BSA-Zr-TMS-10, BSA-Zr-TMS-15, BSA-Zr-TMS-20 and BSA-Zr-TMS-25 are found to be 0.50, 0.72, 1.19, 1.22, 1.31 and 1.34 mmol/g, respectively (Table 1). These values are in agreement with the output of the elemental analysis result shown in Table 1, where the total acidity of the material is increased with respect to the loading of sulphonic acid over B-Zr-TMS. Further, the total acidity of $SO_4^{2-}/ZrO_2$ was measured in six stages and found to be 1.45 mmol/g. These results demonstrate that the functionalization of benzyl group loaded Zr-TMS with sulphonic acid enhances the acidity of the material and consequently the conversion of diphenyl ether to 4-phenoxybenzophenone (4-PBP).

### 3.2. Catalytic testing

The catalytic activity of the synthesized materials was examined in the benzoylation of diphenyl ether with benzoyl chloride to 4-PBP in a batch reactor using nitrobenzene as solvent at 160 °C for 0.5 h. Same reaction was also carried out using Zr-TMS and $SO_4^{2-}/ZrO_2$ for comparison. Results are presented in Table 2.

Under similar reaction conditions, the BSA-Zr-TMS catalysts were more active than Zr-TMS and $SO_4^{2-}/ZrO_2$. The less activity of Zr-TMS (11.7 wt.%) and $SO_4^{2-}/ZrO_2$ (4.6 wt.%) are due to the limited number of acid sites and non-availability of mesoporous nature, respectively. The geometry size of diphenyl ether was found to be 8.99 Å (horizontal), which clearly shows that the diffusion of product either from the pores or the interlayer distance of $SO_4^{2-}/ZrO_2$ is not easy. As evidenced from Fig. 3 (more than 10 wt.% sulphonic acid loading over B-Zr-TMS leads to severe structure collapse), only two functionalized catalysts, BSA-Zr-TMS-5 and -10 were taken into consideration and the results are presented in Table 2. The BSA-Zr-TMS-5 and -10 gave the DPE conversion of 33.7 and 57.5 wt.%, respectively, with 100 wt.% selectivity to 4-PBP. The increase in DPE conversion is attributed to the increase in sulphonic acid loading over B-Zr-TMS. Turn over frequency (TOF, $mol^{-1}\ S\ s^{-1}$) for all the catalysts are calculated as the number of moles of DPE converted per

Table 2
Benzoylation of diphenyl ether using synthesized catalysts[a]

| Catalysts | Conversion of DPE (wt.%) | TOF[b] ($mol^{-1}\ S\ s^{-1)}$) | Product selectivity to 4-PBP (wt.%)[c] |
|---|---|---|---|
| Zr-TMS | 11.7 | – | 100 |
| BSA-Zr-TMS-5 | 33.7 | 21.5 | 100 |
| BSA-Zr-TMS-10 | 57.5 | 29.4 | 100 |
| $SO_4^{2-}/ZrO_2$ | 4.6 | 2.3 | 100 |

[a] Reaction conditions: diphenyl ether (mol) = 0.01; benzoyl chloride (mol) = 0.01; nitrobenzene (ml) = 20; catalyst (g) = 0.5; reaction time (h) = 0.5; reaction temperature (°C) = 160.

[b] TOF is calculated as the number of moles of DPE converted per mole of sulfur per second.

[c] 4-PBP: 4-phenoxybenzophenone.

mole of sulfur per second. TOF for BSA-Zr-TMS-5, BSA-Zr-TMS-10 and $SO_4^{2-}/ZrO_2$ are found to be 21.5, 29.4 and 2.3 $mol^{-1}S\ s^{-1}$, respectively. All these results demonstrate that the substrate needs acidic catalyst with well-defined mesoporous structure for enhanced activity.

## 4. Conclusions

In summary, Zr-TMS has been synthesized with high surface area and functionalized with benzyl sulphonic acid using post-synthetic route by applying the etherification and subsequent sulphonation reactions to get covalently bonded BSA-Zr-TMS ($\equiv Zr–O–CH_2–\Phi–SO_3H$) catalysts. Various amounts of sulphonic acid were loaded over B-Zr-TMS and the maximum amount of sulphonic acid loading was optimized to 9.1 wt.% (input 10 wt.%) without destroying the mesoporous structure of the material. The powder XRD confirms the mesoporous nature of the materials. The $N_2$ adsorption–desorption studies ascribed the high surface area and considerable pore size distribution, which is in general agreement with previous values reported for mesoporous $ZrO_2$. The FT-IR study revealed the successful anchoring of benzyl group and the subsequent functionalization of $–SO_3H$ group. The $NH_3$ TPD measurements showed that the catalysts are acidic in nature with proper acid strength. The synthesized catalysts were used in the benzoylation of diphenyl ether with benzoyl chloride and found to be more active and selective due to their mesoporosity and to an increase in the number of acid sites. Zr-TMS and $SO_4^{2-}/ZrO_2$ were found to be poorly active because of the lower acidic and non-mesoporous nature, respectively. The higher activity of the synthesized materials may be attributed to its higher acidity and mesoporous characteristics.

## Acknowledgements

S.P. acknowledges the CSIR, India for awarding Senior Research Fellowship. The authors are thankful to Miss. Violet, Drs. Seema S. Deshpande and Nalini E. Jacob for their co-operation in characterizing the catalysts.

## References

[1] C.T. Kresge, M.E. Leonowicz, W.J. Roth, J.C. Vartuli, J.S. Beck, Nature 359 (1992) 710–712.
[2] F. Marlow, D. Demuth, G. Stucky, F. Schuth, J. Phys. Chem. 99 (11) (1995) 1306–1310.
[3] M.S. Wong, J.Y. Ying, Chem. Mater. (1998) 10.
[4] Y. Inoue, H. Yamazaki, Bull. Chem. Soc. Jpn. 60 (1987) 891–891.
[5] A. Clearfield, Inorg. Chem. 3 (1964) 146–148.
[6] Z.R. Tian, W. Tong, J.Y. Ying, N.G. Duan, V.V. Krishnan, S.L. Suib, Science 276 (1997) 926–930.
[7] R.A. Boyse, E.I. Ko, Catal. Lett. 38 (1996) 225–230.
[8] (a) T. Jin, T. Yamaguchi, K. Tanabe, J. Phys. Chem. 90 (1986) 4794–4796;
(b) B.H. Davis, R.A. Keogh, R. Srinivasan, Catal. Today 20 (1994) 219–256;
(c) X. Song, A. Sayari, Catal. Rev. Sci. Eng. 38 (1996) 329–412.
[9] Y.Y. Huang, T.J. McCarthy, W.M.H. Sachtler, Appl. Catal. A: Gen. 148 (1996) 135–154.
[10] U. Ciesla, M. Froba, G.D. Stucky, F. Schuth, Chem. Mater 11 (1999) 227–234.
[11] K. Wilson, A.F. Lee, D.J. Macquqrrie, J.H. Clark, Appl. Catal. A: Gen. 228 (2002) 127–133.
[12] F. Mohino, I. Díaz, J.P. Pariente, E. Sastre, Stud. Surf. Sci. Catal. 142 (2002) 1275–1282.
[13] I. Díaz, F. Mohino, J.P. Pariente, E. Sastre, Appl. Catal. A: Gen. 205 (2001) 19–30.
[14] I. Díaz, F. Mohino, J.P. Pariente, E. Sastre, P.A. Wright, W. Zhou, Stud. Surf. Sci. Catal. 135 (2001) 1248–1253.
[15] I. Díaz, F. Mohino, E. Sastre, J.P. Pariente, Stud. Surf. Sci. Catal. 135 (2001) 1383–1390.
[16] I. Díaz, C.M. Alvarez, F. Mohino, J.P. Pariente, E. Sastre, J. Catal. 193 (2000) 295–303.
[17] M. Chidambaram, D. Curulla-Ferre, A.P. Singh, B.G. Anderson, J. Catal. 220 (2003) 442–456.
[18] D. Margolese, J.A. Melero, S.C. Christiansen, B.F. Chmelka, G.D. Stucky, Chem. Mater. 12 (2000) 2448–2459.
[19] J.R. Sohn, S.G. Ryu, Y.I. Pae, S.J. Chol, Bull. Korean Chem. Soc. 11 (1990) 403–406.
[20] U. Ciesla, S. Schacht, G.D. Stucky, K.K. Unger, F. Schuth, Angew. Chem. Int. Ed. Engl. 35 (1995) 541–543.
[21] N.C. Marziano, L.D. Ronchin, C. Tortato, A. Zingales, A.A. Sheikh-Osman, J. Mol. Catal. A: Chem. 174 (2001) 265–277.
[22] A.N. Parvulescu, B.C. Gagea, M. Alifanti, V. Parvulescu, V.I. Parvulescu, S. Nae, A. Razus, G. Poncelet, P. Grange, J. Catal. 202 (2001) 319–323.
[23] P.N. Kuznetsov, L.I. Kuznetzova, A.M. Zhyzhaev, G.L. Pashkov, V.V. Boldyrev, Appl. Catal. A: Gen. 227 (2002) 299–307.
[24] M. Suzuki, S. Ito, T. Kuwahara, Bull. Chem. Soc. Jpn. 56 (1983) 956–957.